GEOMATICS, NATURAL HAZARDS AND RISK
2020, VOL. 11, NO. 01, 2239–2262
https://doi.org/10.1080/19475705.2020.1836040

Taylor & Francis
Taylor & Francis Group

Evaluation of multi-GNSS high-rate relative positioning for monitoring dynamic structural movements in the urban environment

Mosbeh R. Kaloop[a,b,c], Cemal O. Yigit[d,e], Ahmed El-Mowafy[e], Mert Bezcioglu[d], Ahmet A. Dindar[f] and Jong Wan Hu[a,b]

[a]Department of Civil and Environmental Engineering, Incheon National University, Incheon, Korea; [b]Incheon Disaster Prevention Research Center, Incheon National University, Incheon, Korea; [c]Public Works and Civil Engineering Department, Mansoura University, Mansoura, Egypt; [d]Department of Geomatics Engineering, Gebze Technical University, Gebze, Turkey; [e]School of Earth and Planetary Sciences, Curtin University, Perth, Australia; [f]Department of Civil Engineering, Gebze Technical University, Gebze, Turkey

ABSTRACT

Skyscrapers cause both limited sky-view and multipath error when using Global Navigation Satellite System (GNSS) measurements for monitoring structural movements. To reduce multipath errors, cut-off elevation angle can be set to a high value such as 30°−40°. However, in the case of employing high cut-off elevation angles, the use of GPS only may not provide adequate positioning solutions. To overcome this problem, Galileo and GLONASS observations are combined with GPS observations. This study experimentally investigates the contribution of multi-GNSS for studying the effects of different cut-off elevation angles on the accuracy of high-rate GNSS results for detecting characteristics of dynamic motions for structural health monitoring (SHM). The filtration design, noise level and Signal-to-Noise Ratio (SNR) of high-rate GNSS measurements of GPS-only, GPS/Galileo, GPS/GLONASS and GPS/GLONASS/Galileo are assessed for different cut-off elevation angles. The results demonstrate that the SNR of GNSS solutions for GPS/GLONASS and GPS/GLONASS/Galileo is the highest, which signifies their use in SHM. The accuracy of the dynamic movements of structures can be attained to 2 mm, on average, using multi-GNSS measurements even when using high cut-off elevation angles up to 40°. The precision of GPS/GLONASS and GPS/GLONASS/Galileo systems with different cut-off elevation angles was high when referenced to LVDT.

ARTICLE HISTORY
Received 28 August 2020
Accepted 5 October 2020

KEYWORDS
High-rate GNSS; cut-off elevation; multipath; structural health monitoring; Dynamic motions

CONTACT Jong Wan Hu jongp24@inu.ac.kr

Supplemental data for this article is available online at https://doi.org/10.1080/19475705.2020.1836040.

1. Introduction

Nowadays, structural health monitoring (SHM) for tall buildings in metropolitan cities is necessarily required for structures safety. Different sensors, such as displacement and accelerometer sensors, are used to extract the characteristics, amplitude, damping and frequency of dynamic motions of structures. The Global Navigation Satellite System (GNSS) is one of these sensors, which can measure accurate positions of the monitoring points on structures in two or three dimensions. The relative GNSS monitoring system is regularly employed to precisely extract dynamic behaviours of structures. The precise point positioning (PPP) method has been investigated and improved for dynamic analyses of structures (Yigit 2016; Kaloop et al. 2018, 2019; Paziewski et al. 2019, 2020; Yigit et al. 2020). The methods that used GNSS positioning for dynamic analysis of structures can be found in Larocca et al. (2005), Moschas and Stiros (2014), Kaloop et al. (2017), Yu et al. (2018), Shen et al. (2019), Yu et al. (2020). For instance, Schaal and Larocca (2002) applied the phase-residual method for estimating dynamic movements of structures based on GPS observations. Souza and Negri (2017) used multipath effects for estimating movement of structures without installing a receiver on it. Paziewski et al. (2018) proposed a GNSS phase direct signal-processing approach technique using real-time kinematic (RTK) and PPP methods for determining dynamic displacements. They assessed the usability of multi-constellation GNSS signals for high-rate dynamic displacement detection by focusing on both the processing methodology and practical performance evaluation. Their results based on comparative analysis confirmed that all the presented method can be considered as powerful tools for detecting high-rate millimeter-level displacements. Shen et al. (2019) summarized the methods that can be used for estimating the structures movements based on GNSS-only and integrated sensors with GNSS; such as, variometric approach, phase-residual method and signal-processing method. Dabove and Pietra (2019) used the single-baseline RTK positioning to estimate structural displacements using geodetic-grade GNSS receivers and smartphone. The obtained accuracy from GNSS positioning approaches was at several mm. Paziewski et al. (2020) proposed a method based on the multi-baseline solution for estimating seismic movements by using GNSS positioning. Also, high precision dynamic performance was achieved using the relative and PPP-GNSS methods. Likewise, real-time GNSS measurements were observed at a high-rise building in Madrid, Spain, 2016, to detect and evaluate the building performance under wind load effects. A geodetic network was used (Olmo et al. 2016). The construction of La Costanera tower in Santiago, Chile, was monitored using RTK GNSS, and the results showed that this technique is suitable for monitoring structures during and after construction periods (da Silva et al. 2018). The monitoring of the W tower movements in Guangzhou, China, *via* GNSS, was carried out and the accuracy of the positions was at the millimetre-level (Zhang et al. 2018). More studies on using GNSS for monitoring structure movements can be found in Shen et al. (2019), Kaloop et al. (2017, 2019), Yu et al. (2020), Yigit and Gurlek (2017). However, some errors affect the GNSS accuracy for structure monitoring; multipath error, in particular, is still the primary source of error (Shariati et al. 2019; Yu et al. 2018).

GNSS observations are generally collected with 10°–15° cut-off elevation angle to eliminate or decrease multipath error and the troposphere delay in case of non-differencing techniques such as PPP (Li et al. 2018; El-Mowafy et al. 2020). In this case, the GPS is used in different engineering applications (Ruotsalainen and Kuusniemi 2013; Paull et al. 2014) since the number of satellites in the open-sky view is sufficient to extract structural movements with an acceptable accuracy level. Furthermore, the open-sky view provides a small value of satellite position dilution of precision (PDOP), which affects the position accuracy of GNSS receivers (Guo et al. 2020). In SHM, the GPS was used to monitor structures that have an open-sky view; for instance, the movement of many long-span bridges (Kaloop and Kim 2014; Han et al. 2016; Gökalp and Taşçı 2009). Moreover, it was used to assess movements of tall constructions that have an open-sky view (Górski 2017; Sofi et al. 2018). On the other hand, in the areas that comprise crowded buildings, such as metropolitan areas, signal obstruction and multipath affect the accuracy of GPS observations for SHM even when using high cut-off elevation angles.

It is well known that the increase of the cut-off elevation angle influences the number of GPS satellites observed and the achieved positioning accuracy. Therefore, the use of a combined GNSS, such as GPS/GLONASS, GPS/Galileo, GPS/BDS, GPS/GLONASS/Galileo, GPS/GLONASS/BDS (BeiDou Navigation Satellite System), GPS/Galileo/BDS and GPS/GLONASS/Galileo/BDS improves the positioning accuracy of GPS-only solutions. Single or dual GNSS, with 10–30 satellites were successfully used for improving the reliability of the positioning system for SHM, particularly in constrained and harsh environments (Liu et al. 2019; Pan et al. 2014; Han et al. 2018). Consequently, the cut-off elevation angle can be increased (Liu et al. 2019). Xi et al. (2019) evaluated the integration of GPS, BDS and GLONASS for the evaluation of bridge movements with rising the cut-off elevation angle up to 40°, and they concluded that the integrated GNSS systems could be used to improve detection of dynamic movements using high cut-off elevation angles. Paziewski and Sieradzki (2017) compared RTK positioning performance of GPS-only, BDS-only and combined GPS and BDS observations with different cut-off angles, from 5° to 40° with 5° step. The assessment was performed in both ambiguity resolution and coordinate estimation domains. The authors demonstrated that GPS and BDS combined positioning has advantage over single GPS and single BDS solution for ambiguity resolution, especially in harsh observing conditions. Most recently, Xi et al. (2021) integrated GPS, BDS and GLONASS observations for monitoring a bridge movement at different cut-off elevation angles. Their results demonstrated that the bridge movement characteristics could be derived with an acceptable accuracy at 40° cut-off elevation angle. Teunissen et al. (2014) assessed the performance of integrated GPS with BDS satellite systems for estimating RTK positioning with cutting elevation angles from 10° to 40°; and their results showed that with the multi-GNSS system, much greater than customary cut-off elevation angles can be applied; and this will increase the use of multi-GNSS systems in constrained atmospheres. Ge et al. (2019) evaluated the single-frequency-PPP using multiple GNSS systems with cut-off elevation angles, from 10° to 40°, and they found the performance of the long-term stability worsen when increasing the cut-off elevation angle. Liu et al. (2019) used a selection satellite

system based on ambiguity dilution of precision (ADOP) to improve positioning using the single-frequency single-epoch multiple GNSS with different cut-off elevation angles. Their results signified the use of a minimum number of high-elevation angle satellites based on a proposed method with a success rate close to 100%, consequently improving the receivers positioning efficiency. Blanco-Delgado and Nunes (2010) and Zhang et al. (2013) applied a method for selection of satellites based on their geometry to improve positioning results. The effectiveness of cut-off elevation angle on the accuracy of GNSS positioning with a focus on the computational time was studied in Luo et al. (2020), Ou et al. (2014), Abedi et al. (2020). However, so far, the application of different GNSS combinations (such as those of GPS, GLONASS and Galileo) with high cut-off elevation angles has not been thoroughly investigated for extracting accurate dynamic characteristics of structures and SHM. These points are addressed in our paper.

The main motivation of this study is to investigate the benefit, efficiency and usability of high-rate GNSS multi-constellation with high cut-off elevation angle for SHM and find a suitable method for estimating the dynamic behaviours of engineering structures in urban areas, such as high-rise or skyscraper, especially those surrounded by obstacles causing limited sky view and multipath error for GNSS observations. The positioning performance of the GPS-only, GPS/Galileo, GPS/GLONASS and GPS/GLONASS/Galileo combinations were analyzed for different cut-off elevation angles, such as 10°, 20°, 30° and 40°. LVDT data were taken as a reference for time and frequency domain analyses.

This work is organized as follows. In Section 2, experimental dataset and processing strategies are presented. Section 3 demonstrates the experimental results obtained from GPS-only and the multiple GNSS, GPS/Galileo, GPS/GLONASS and GPS/GLONASS/Galileo observations. The performance of these combined GNSS is discussed and experimentally evaluated in detail for extracting accurate structures behaviours under different cases of shaking loads. Different dynamic amplitudes and frequencies are investigated in this study. Furthermore, the results of different cut-off elevation angles, 10°, 20°, 30° and 40°, are evaluated and assessed. Our conclusions are presented in Section 4.

2. Experiment description and GNSS data processing

2.1. Experiment description

In this study, a shake table that can produce a sinusoidal harmonic movement with different frequencies and amplitudes was used (Figure 1). The shake table has a flat plate that can be subjected to a maximum displacement of ±190 mm. Four GNSS receivers were mounted on it to capture harmonic oscillations (cf. Figure 1). An electric motor was attached to the shake table and used to generate dynamic movements. The stability of the table was maintained using weights placed on both sides of the platform to prevent unwanted oscillations when studying high-rate movements. The position of the table on the frame rails was controlled by software running on a Windows computer platform; where the controller verifies the position information

Figure 1. Shake table and the GNSS receivers attached on it.

using an LVDT that measures the position of the table with mm precision, collecting 100 samples per second (100 Hz).

Five dual-frequency CHC I80 GNSS receivers were used to test the performance of high-rate GNSS positioning for SHM under different elevation cut-off angle. The four GNSS receivers mentioned above that were mounted on the shake table to collect GNSS observations with 10°, 20°, 30° and 40° satellite cut-off angle. The fifth GNSS receiver was installed approximately 60 m away from the shake table as a base-station for the relative GNSS positioning. GPS (L1 and L2), GLONASS (L1 and L2) and Galileo (E1 and E5) satellite observations were collected at a 20 Hz (0.05 s) sampling rate. The experiment was carried out on 4 April 2019, at the Gebze Technical University and lasted approximately 2 h. The experiment was conducted under open-sky and with calm weather conditions. In order to evaluate the performance of the relative positioning under different satellite elevation cut-off angle, a broad harmonic oscillation set with different amplitudes and frequencies was generated to cover a wide range of possible structural movements. Six experiments with different harmonic oscillations were selected and performed where GNSS results were compared with reference LVDT data. Table 1 summarizes these harmonic oscillation events with their frequency and amplitude values. Furthermore, superimposed harmonic oscillation with three frequencies, namely 0.8, 3.4 and 7.6 Hz, were generated.

2.2. GNSS data processing

2.2.1. Processing method

The GNSS relative positioning data were processed using the open-source software RTKLIB 2.4.3 b33 (Takasu and Yasuda 2009). Dual-frequency measurements were used. Double differences of the carrier phase signals were used to eliminate the effect of the spatially correlated troposphere and ionosphere delays and orbital errors, in addition to the satellite and receiver clock offsets. A GNSS integer-ambiguity fixed solutions were estimated. The parameters used in the solution are described in Table 2.

Table 1. Frequency and amplitude of the selected events in this study.

	Oscillation amplitude	
Oscillation frequency (Hz))	5 mm	10 mm
0.1	Event 1	Event 2
0.6	Event 3	Event 4
1.5	Event 5	Event 6

Table 2. The settings of RTKLIB for the GNSS relative solution.

Positioning mode	Kinematic
Frequency	GPS (L1 and L2) GLONASS (L1 and L2) GALILEO (E1 and E5)
Filter type	Combined (smoother combined solution with forward and backward filter solutions)
Data sampling period/frequency	0.05 s/20 Hz
Cutoff elevation angle	10°, 20°, 30° and 40°
Observations	Carrier phase and code
Integer-ambiguity resolution	Fixed (ambiguities are estimated and fixed)
Min. ratio to fix ambiguity	2.0
Reject threshold of GDOP	20

2.2.2. Filtering the obtained GNSS positions time series

At this step, the GNSS coordinates are transferred to a local coordinate system defined by one axis aligned along the movement direction of the testing plate and another axis is perpendicular to it; such that the position along the direction of movement was calculated and evaluated. After that, any position outlier was detected by comparing the position error with a threshold determined by three times the standard deviation. The dominant frequency was determined using spectral interval analysis, which can be used to estimate the statistically and structurally significant information of structures movements. Here, the observation noise and multipath error can be detected in the frequency domain and are used to define the frequency band of structure movements. Multipath effect may reach up to several centimetres, which adversely affects the kinematic position accuracy (Paziewski et al. 2019). The instantaneous impact of multipath is typically merged with phase noise. The longer-term multipath effects have relatively long periods (several minutes and more) and low frequency with respect to the frequency band of structure movements. This implies that multipath effect can be effectively mitigated with a high-pass, band-pass or band stop filtering to obtain high-accuracy displacements (Paziewski et al. 2019, Kaloop et al. 2019). In this study, an 11-order Chebyshev band-pass filter with appropriate parameters for each event was implemented. The filter was designed using band-pass frequencies and pass- and stop-band ripples 1 and 20 dB, respectively. For stability of the filter, the zero-pole-gain filter parameters were converted to second-order sections (Shenoi 2005). Figure 2 illustrates the filter of the superimposed harmonic oscillation. Based on the filter parameters, noises corresponding to the frequencies that were out of the pass-band range frequencies defined previously were

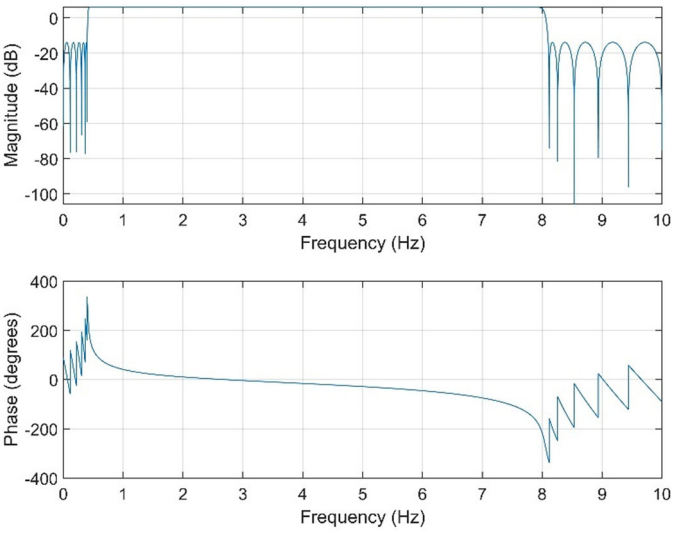

Figure 2. Design of the 11-order Chebyshev filter used to de-noise the GNSS apparent oscillation of superimposed harmonic signal.

removed. Various studies applied low-pass or band-pass/high-pass filters to remove noises or subtract frequencies from GPS/GNSS or accelerometer time series (Górski 2017; Moschas and Stiros 2011). Here, for estimating the amplitude and frequency of the oscillations, first, filtration processing was designed to remove the noises; then, the Fast Fourier Transformation (FFT) was used.

3. Results and discussion

3.1. Assessment of some GNSS positioning parameters

Figure 3 depicts the average number of satellites observed during the six experiments carried out in this study and Figure 4 shows the sky-view plot during these experiments. During the time of the test, the number of GLONASS satellites observed was more than the number of Galileo satellites. Therefore, the contribution of GLONASS satellites to GPS observations is higher than that of Galileo satellites for the 40° cut-off elevation angle. When using the three GNSS, it can be observed that the satellite numbers with cut-off elevation angle 10° were decreased by 25%, 40% and 60% on average, relative to the number of satellites, in the cases of using cut-off elevation angles of 20°, 30° and 40°, respectively.

As an example, Figure 5 shows the average PDOP values observed during all the studied events. The best PDOP under 10°, 20° and 30° cut-off elevation angles were obtained by multi-GNSS observations. GPS/Galileo under the 20° and 30° cut-off elevation angle has larger PDOP values compared to GPS/GLONASS. However, under the 40° cut-off elevation angle, the GPS/Galileo combination has poor geometry due to bad constellation geometry. The PDOP values shown are equal on average for the GPS/GLONASS and GPS/Galileo/GLONASS under 40° cut-off elevation angle.

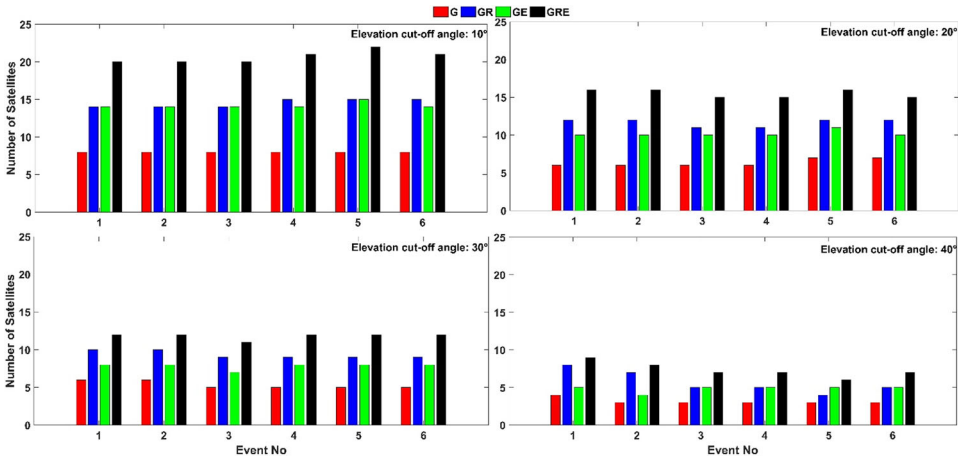

Figure 3. The number of GNSS satellites for the selected events for different elevation cut-off angles (10° top-left, 20° top-right, 30° bottom-left, 40° bottom-right) (G: GPS, GR: GPS + GLONASS, GE: GPS + Galileo, GRE: GPS + GLONASS + Galileo).

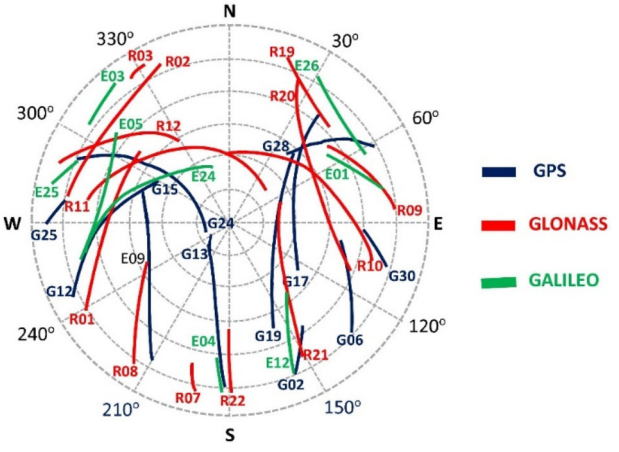

Figure 4. Sky-view plot during testing.

3.2. Time-domain processing evaluation

This section evaluates the performance of unfiltered and filtered GNSS results for three dynamic behaviours, namely; low, medium and high structural movements with different frequencies and amplitudes presented by the six tested events. Appendices A and B (see Supplementary material) include more results for the events. Here, events 1–6 for multi-GNSS were evaluated at 10°, 20°, 30° and 40° cut-off elevation angles. As mentioned earlier, the LVDT data were used as a reference trajectory to assess the GNSS results. The LVDT measures the position of the table at the mm level with 100 samples per second (100 Hz). Figure 6 illustrates the unfiltered and filtered (smoothed) multi-GNSS results for events 1 (low frequency and amplitude event) and 6 (high frequency and amplitude event) for the GPS-only at 10° cut-off elevation angle and GPS/Galileo/GLONASS at 40° cut-off elevation angle, respectively, as the two extreme examples. In addition, Figure 7 and Appendix A (see Supplementary

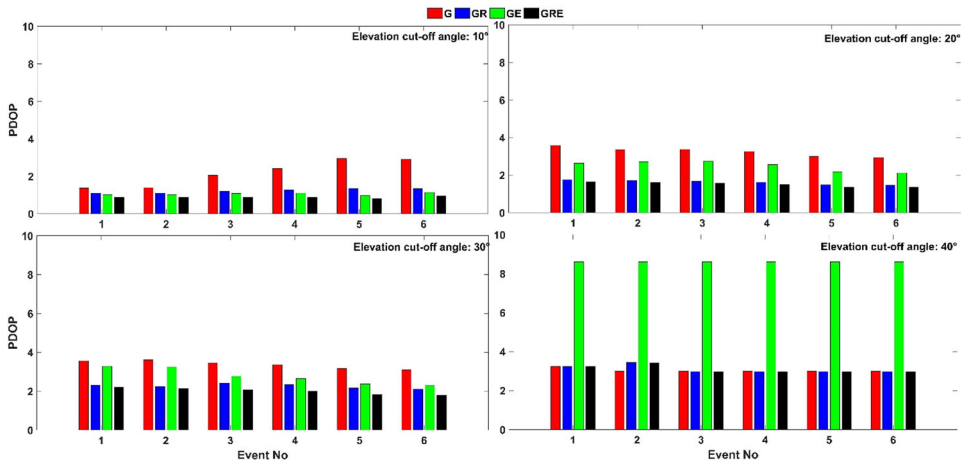

Figure 5. The PDOP values for the selected events at different cut-off elevation angles (10° top-left, 20° top-right, 30° bottom-left, 40° bottom-right).

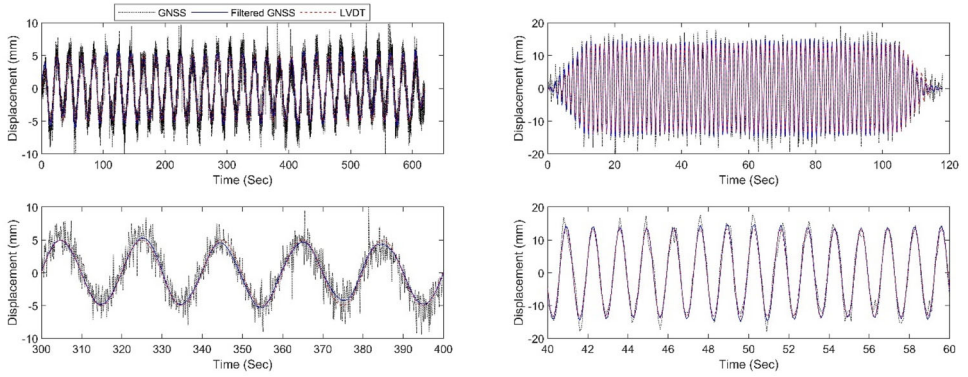

Figure 6. LVDT, filtered and unfiltered (top), zoom in (bottom), GNSS results for the (a) event 1 (for GPS-only) and (b) event 6 (for GPS/Galileo/GLONASS).

material) present the accuracy improvement of filtered GNSS results in terms of root mean square error (RMSE) and the correlation between smoothed (filtered) GNSS signals and LVDT, respectively. Figure 8 shows the SNR of the whole events before and after applying the filter processing. The SNR $= 20\log(S/N)$, where S and N are the sums of squared magnitudes of measured signals (structure movements) and their noises (the variation between structure movements that measured by GNSS and LVDT techniques). The RMSE and SNR values of the GNSS results were evaluated relative to those from the LVDT. More results can be seen in Appendix A (see Supplementary material).

From Figures 6–8, it can be shown that the noise level and RMSE increases with increasing the cut-off elevation angle for all GNSS combinations. For instance, the RMSE of movements increased by 63.7% when comparing their values at 10° and 40° using GPS/GLONASS/Galileo case at event 1. In the same time, the SNR value decreased by 42.9% for the same event. Figure 7 shows the RMSE of both filtered

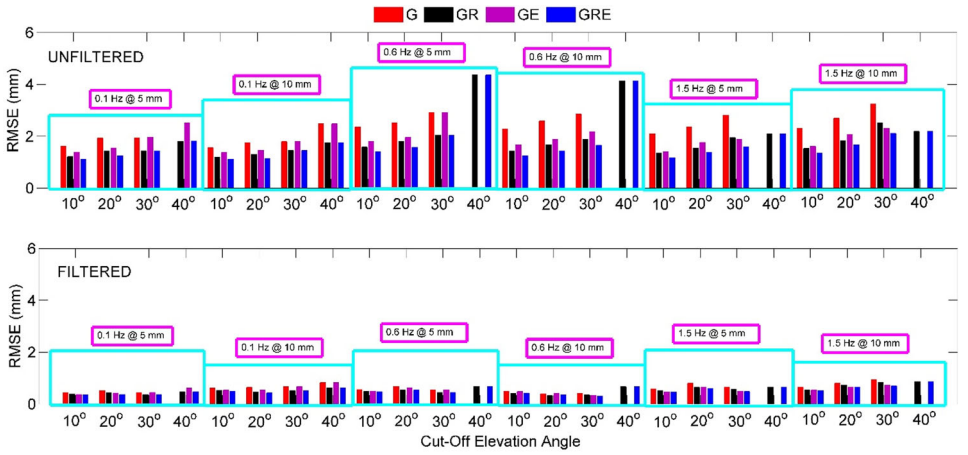

Figure 7. Accuracy (RMSE) assessment of the GNSS results before (top panel) and after (bottom panel) applying the filter process at different frequencies (0.1–1.5 Hz) and amplitudes (5–10 mm).

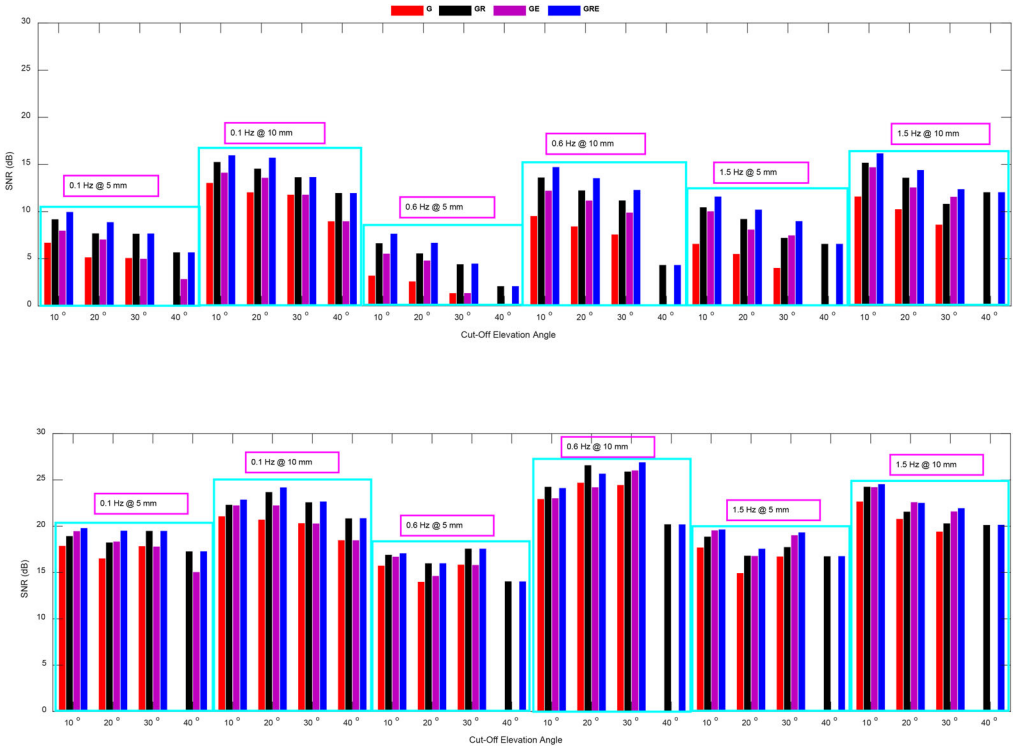

Figure 8. SNR of the unfiltered (top) and filtered (bottom) GNSS results for the events.

and unfiltered GNSS results. In all events/cases, the RMSE values of unfiltered GNSS results increase with increasing the cut-off elevation angle. The figure clearly reveals the benefit of the integrated GPS/GLONASS, GPS/Galileo and GPS/GLONASS/Galileo. Note that in all events and all cut-off elevations, the RMSE of the integrated GPS/GLONASS/Galileo is smaller than GPS-only, GPS/GLONASS and GPS/Galileo

due to the use of more satellites and the improvement in the satellite geometry. In case of the 40° cut-off elevation angle, GPS/GLONASS and GPS/GLONASS/Galileo still provide positioning for all events while GPS-only and the integrated GPS/Galileo do not produce positioning solution for some events. After filter implementation to GNSS results, the RMSE values of all satellite combinations improve significantly for all cut-off elevations, as presented in Figure 7. Differences between the RMSE values of filtered low and high cut-off elevations get smaller when compared to those of the unfiltered low and high cut-off elevations. Moreover, the RMSE differences between GPS-only and all other combinations get closer after filtering. However, GPS/GLONASS/Galileo combination for all events and all cut-off elevation angles still provide the most accurate results (see Appendix A, see Supplementary material). As the results of both unfiltered and filtered GPS/GLONASS and GPS/GLONASS/Galileo combined systems are very promising, it can be concluded that a combined system would allow the use of higher cut-off elevations.

To further analyze the performance of all GNSS solutions the SNR values are presented in Figure 8. The SNR values of 40° cut-off elevation angle were lower than that for the 10° cut-off elevation angle. This was expected as the number of satellites should be small when using a 40° cut-off elevation angle, as well as the PDOP value, which affects the positioning accuracy. In addition, the noise level of low amplitude events (5 mm) was high compared with the large amplitude events, see Figure 8. This indicates that the measurement noises are low with large amplitude movements. Furthermore, the SNR for GPS/GLONASS and GPS/GLONASS/Galileo combinations were better than the other cases for all events before removing the noise. In addition, from Figure 8, it can be shown that at a 40° cut-off elevation angle, the movements cannot be detected by using GPS-only and GPS/Galileo because the number of GPS and Galileo satellites is not enough for positioning. This reveals that the GPS/GLONASS combination provides a more continuous and accurate solution than GPS/Galileo combination in this study as shown in Figure 1 where the number of Galileo satellites was less than that of GLONASS.

The use of the filter has improved the GNSS results as presented in Appendix A (see Supplementary material) and Figures 6–8. The correlation between the filtered GNSS results and LVDT signals is high, more than 0.99 for all events, for all cut-off elevations and all GNSS combinations. The amplitude of filtered movements is lower than that of the unfiltered movements, which were contaminated by noises, as presented in Figure 6. The use of the filter increased the accuracy of GNSS results for all GNSS systems and cut-off elevation angles by 70%, on average, in terms of the RMSE, as presented in Figure 7 and Appendix A (see Supplementary material). Furthermore, the RMSE of GNSS observations at 40° for the GNSS movements of 0.6 Hz with 5 mm and 10 mm has improved by 84.5% and 83.9%, respectively. This indicates the effectiveness of the filter in detecting the effects of the high noise. In addition, from Figure 8, it can be observed that the level of noise was decreased by 110.67%, 128.47%, 238.22% and 281.29%, on average, for the 10°, 20°, 30° and 40° cut-off elevation angles, respectively. Furthermore, the improvement of SNR is high for GPS/GLONASS and GPS/GLONASS/Galileo combinations, especially at 40° cut-off elevation angle (see Figure 8).

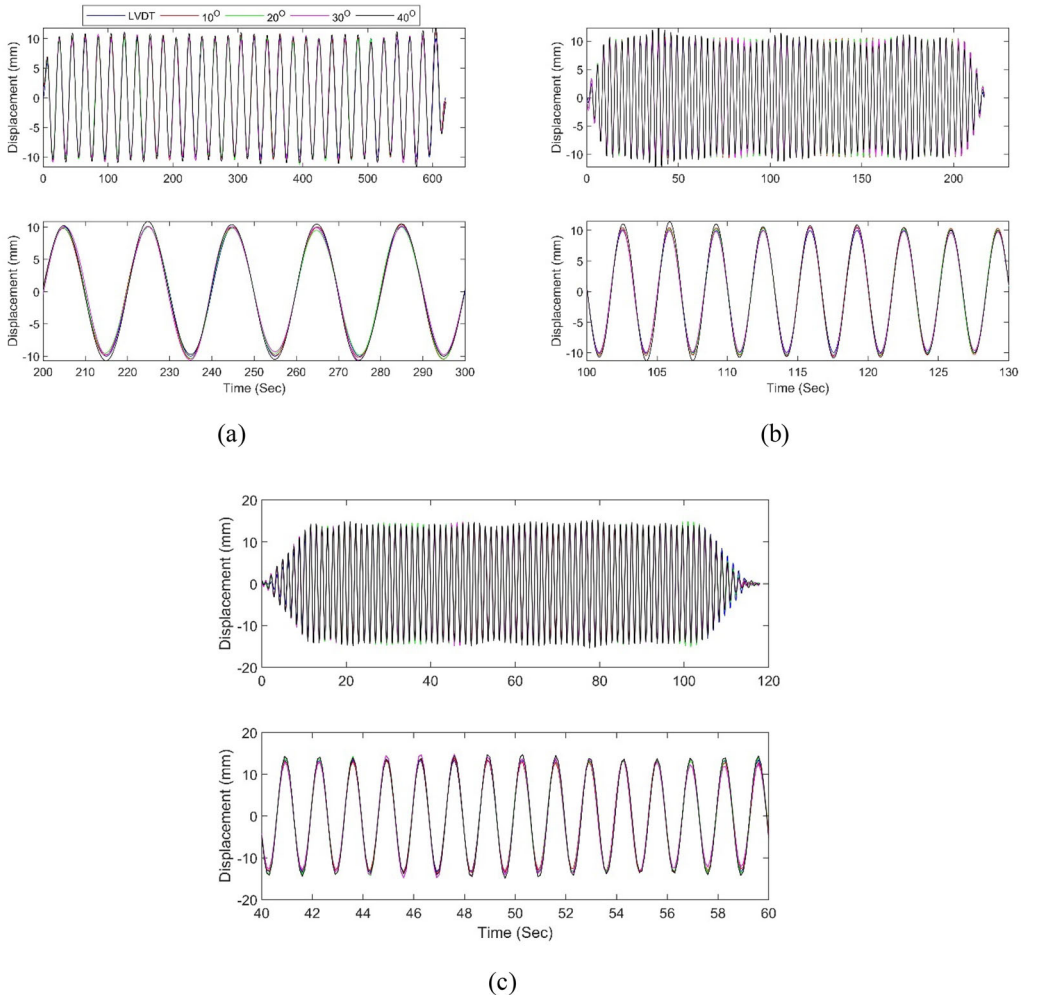

Figure 9. Smoothed signals (top-whole data and bottom-zoom in) for the (a) event 2; (b) event 4 and (c) event 6 for the GPS/GLONASS/Galileo case.

Figure 9 presents the filtered GNSS signals under different cut-off elevation angles for events 2, 4 and 6. The correlation between time series amplitudes of signals at different cut-off elevation angles is also high, 0.98 on average, as presented in Figure 9. This indicates that the GNSS can be accurately used to detect the time series of the amplitudes of structural movements. Besides, the maximum error of the filtered signals at different cut-off elevation angles for the GPS/GLONASS/Galileo was 2 mm, on average, relative to LVDT. Thus, the band-pass filter is a powerful tool that can be used to decrease the noise level caused by high cut-off elevation angles. As a result, it can be concluded that the band-pass filter can be used to estimate accurate signal performances in the time domain for different cut-off elevation angles with different multi-GNSS. A limitation of this kind of filters is that the dominant frequency of monitoring structures should be known in advance through the use of finite element models or accurate dynamic measurements, such as acceleration measurements.

Table 3. Dynamic performance (amplitude and relative displacement change with respect to LVDT) of different GNSS combinations with different cut-off elevation angles.

		10°		20°		30°		40°		LVDT
Events	Method	Amp (mm)	Relative change (%)	Amp (mm)	Relative change (%)	Amp (mm)	Relative change (%)	Amp (mm)	Relative change (%)	Amp (mm)
1	G	4.95	0.69	5.06	3.01	4.94	0.53	–	–	4.91
	GR	5.05	2.71	5.02	2.18	4.89	0.43	5.20	5.86	
	GE	5.00	1.85	5.08	3.42	4.94	0.47	5.29	7.76	
	GRE	5.07	3.09	5.05	2.73	4.86	1.08	5.20	5.84	
2	G	10.00	1.78	10.70	8.95	10.12	3.04	10.60	7.93	9.82
	GR	10.11	2.94	9.93	1.09	9.99	1.76	10.37	5.59	
	GE	10.00	1.79	10.10	2.84	10.13	3.15	10.60	7.93	
	GRE	10.10	2.84	9.97	1.56	9.97	1.51	10.37	5.59	
3	G	5.02	6.41	5.19	10.03	4.50	4.60	–	–	4.72
	GR	4.97	5.32	4.99	5.92	4.66	1.27	4.72	0.00	
	GE	4.97	5.35	5.20	10.37	4.49	4.86	–	–	
	GRE	4.95	4.98	5.06	7.21	4.62	2.02	4.72	0.04	
4	G	9.98	5.37	9.88	4.35	9.49	0.19	–	–	9.47
	GR	9.94	4.94	9.77	3.23	9.70	2.41	9.85	3.99	
	GE	10.01	5.74	9.96	5.23	9.51	0.42	–	–	
	GRE	9.96	5.16	9.86	4.15	9.63	1.70	9.84	3.98	
5	G	5.73	0.19	6.39	11.25	5.98	4.16	–	–	5.74
	GR	5.80	0.98	6.26	9.09	6.03	5.11	6.09	6.17	
	GE	5.74	0.05	6.24	8.66	5.74	0.04	–	–	
	GRE	5.78	0.63	6.20	8.00	5.83	1.52	6.09	6.15	
6	G	10.65	3.45	11.62	5.35	11.30	2.45	–	–	11.03
	GR	10.94	0.82	11.59	5.08	11.44	3.72	11.66	5.71	
	GE	10.86	1.54	11.42	3.54	10.98	0.45	–	–	
	GRE	10.95	0.73	11.48	4.08	11.12	0.82	11.66	5.71	

Therefore, a benchmark solution should be studied and evaluated for different cut-off elevation angles with different multi-GNSS when monitoring behaviours of real structure movements.

3.3. Frequency-domain processing evaluation

In this section, the performance of the GPS-only, GPS/GLONASS, GPS/Galileo and GPS/GLONASS/Galileo combinations are evaluated in the frequency domain. Table 3 presents the FFT amplitude and relative change of different GNSS combinations for different cut-off elevation angles for the six events and the LVDT, similar to Section 3.1. Figure 10 illustrates the dynamic properties of the different GNSS combinations at the 10° cut-off elevation angle of event 3 as a representative example. The changes relative to LVDT were estimated. The frequencies of multi-GNSS of all events were the same as that extracted from LVDT. Furthermore, the correlation of the signals between LVDT and filtered GNSS combinations are high (0.98, on average) for all events and for different cut-off elevations, as seen in Figure 10 and Appendix B (see Supplementary material). This reveals that the power contents of GNSS estimated movements are almost the same from the LVDT. Thus, the GPS-only, GPS/Galileo, GPS/GLONASS and GPS/GLONASS/Galileo can be safely used to extract the frequency contents of structural movements.

The movement amplitude calculated by FFT shows that its relative change is small for all events. From Table 3, Appendices A and B (see Supplementary material), the average relative differences between LVDT and the GPS-only, GPS/GLONASS, GPS/

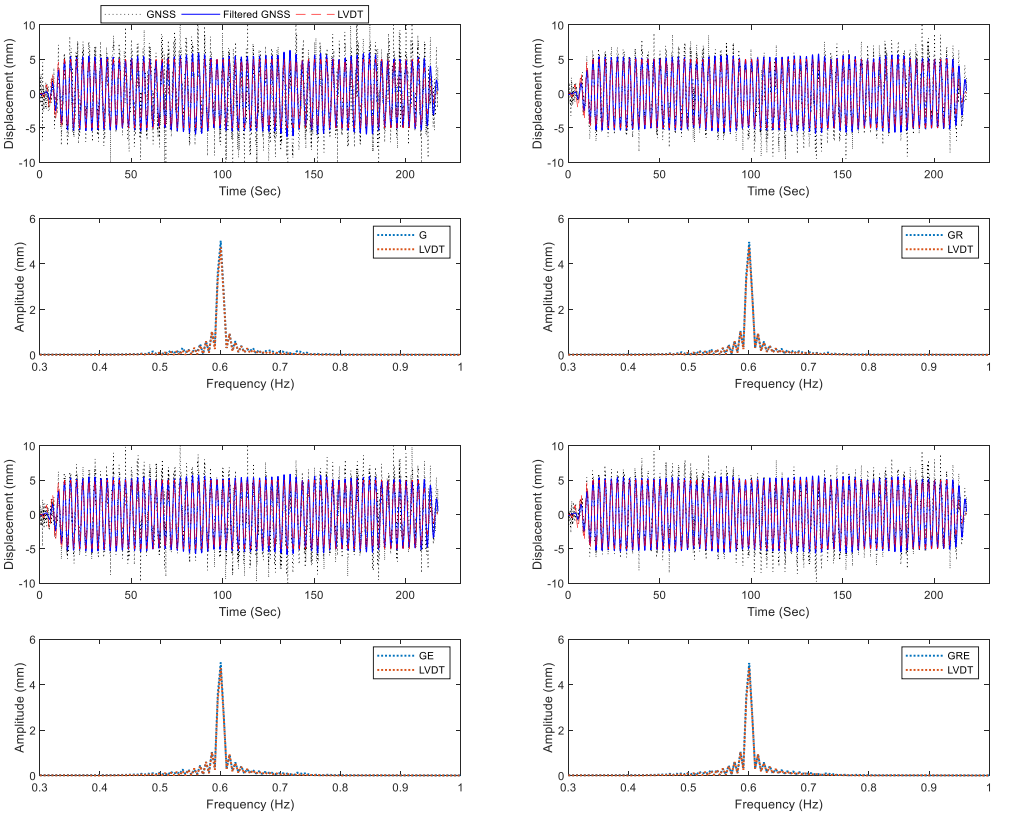

Figure 10. Dynamic characteristics (displacements, amplitudes with frequencies) of structural movements for the event 3, with 10° cut-off elevation angle (G: top-left, GR: top-right, GE: bottom-left, GRE: bottom-right).

Galileo and GPS/GLONASS/Galileo at the 10° cut-off elevation angle for all events are 2.98%, 2.95%, 2.72% and 2.90%, respectively. In addition, the standard deviations of the corresponding relative changes are ±2.53%, ±1.90%, ±2.29% and ±1.97%, respectively. Thus, the result of using a GPS/GLONASS combination is slightly better than when using GPS/GLONASS/Galileo combinations. Moreover, during the test period, where a smaller number of Galileo satellites were observed than that of GLONASS, the performance of GPS/GLONASS is relatively better than GPS/Galileo for extracting the dynamic movements. Here, it should be mentioned that the average change of movement amplitudes for the GPS-only is higher than its combinations with other GNSS for higher cut-off elevation angles (see Appendix B, see Supplementary material). The average relative change of the amplitude for the combined three GNSS was 2.90% and 4.55% for the 10° and 40° cut-off elevations, respectively. The maximum relative change of all events for the GPS-only, GPS/GLONASS, GPS/Galileo and GPS/GLONASS/Galileo are 8.61%, 7.83%, 8.51% and 6.78%, respectively. These results denote that the use of GNSS combinations improves the accuracy of detecting dynamic movement characteristics of structures.

Furthermore, Figure 11 demonstrates a comparison between multi-GNSS systems for event 2 and event 5, as examples, at 10° cut-off elevation angle. From Figures 10

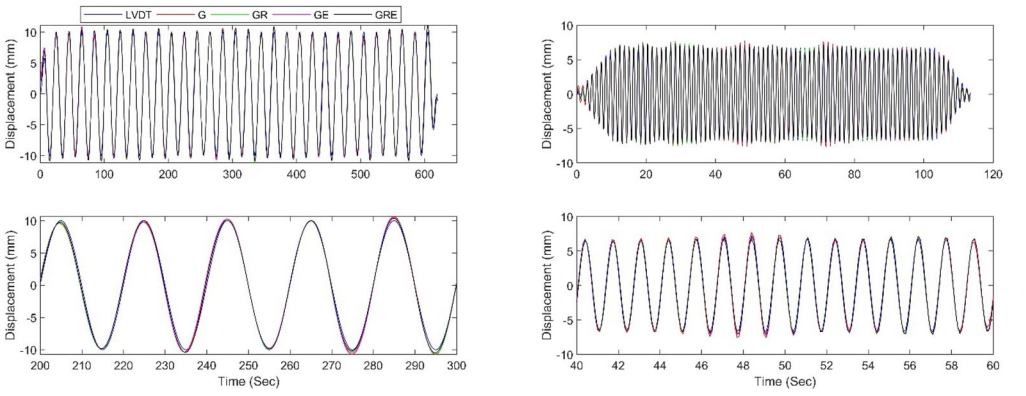

Figure 11. Time series of filtered and unfiltered (top) with zoom in (bottom) of (a) event 2 and (b) event 5 (using a 10° cut-off elevation angle).

and 11, and Appendix B (see Supplementary material), it can be observed that the correlation between LVDT and filtered multi-GNSS signals is high (greater than 0.99 for all events); and is higher for all system combinations than that generated by GPS-only. Furthermore, the performances of GPS/GLONASS and GPS/GLONASS/Galileo combinations were shown the best with higher cut-off elevation angle to estimate the dynamic amplitude and frequency of structural movements (see Appendices A and B, see Supplementary material).

In conclusion, from these results, it can be noted that the performance of GPS/GLONASS/Galileo is the best to estimate the dynamic characteristics of structures since the distribution and number of satellites allow this combination to detect accurate dynamic parameters. The signal powers and amplitudes are shown highly correlated, and the relative changes are low with the LVDT results.

Moreover, in general, it is known that the low elevation satellites are influenced by the residual tropospheric delays and multipath errors; thus, the accuracy of the positioning solution is affected by these errors. Consequently, increasing the number of satellites for multi-GNSS systems with rising cut-off elevation angles could improve positioning; since the PDOP values can be reduced to an acceptable level, as presented in the above sections.

From Table 3, the percentage of the average relative changes for all events and all cut-off elevation angle cases for the GPS-only, GPS/GLONASS, GPS/Galileo and GPS/GLONASS/Galileo combination are 5.14%, 3.60%, 4.45% and 3.38%, respectively. These results indicate that the combined GPS/GLONASS/Galileo gives slightly better SHM performance than GPS-only, GPS/GLONASS and GPS/Galileo. In the case of using a 10° cut-off elevation angle, there is no significant difference between the four combinations. However, GPS/GLONASS and GPS/Galileo give more accurate results than GPS-only for 20°, 30° and 40° cut-off elevation angle whereas GPS/GLONASS/Galileo provide the best and more accurate results. According to results of the relative changes, when comparing results from different cut-off elevation angles, the 30° cut-

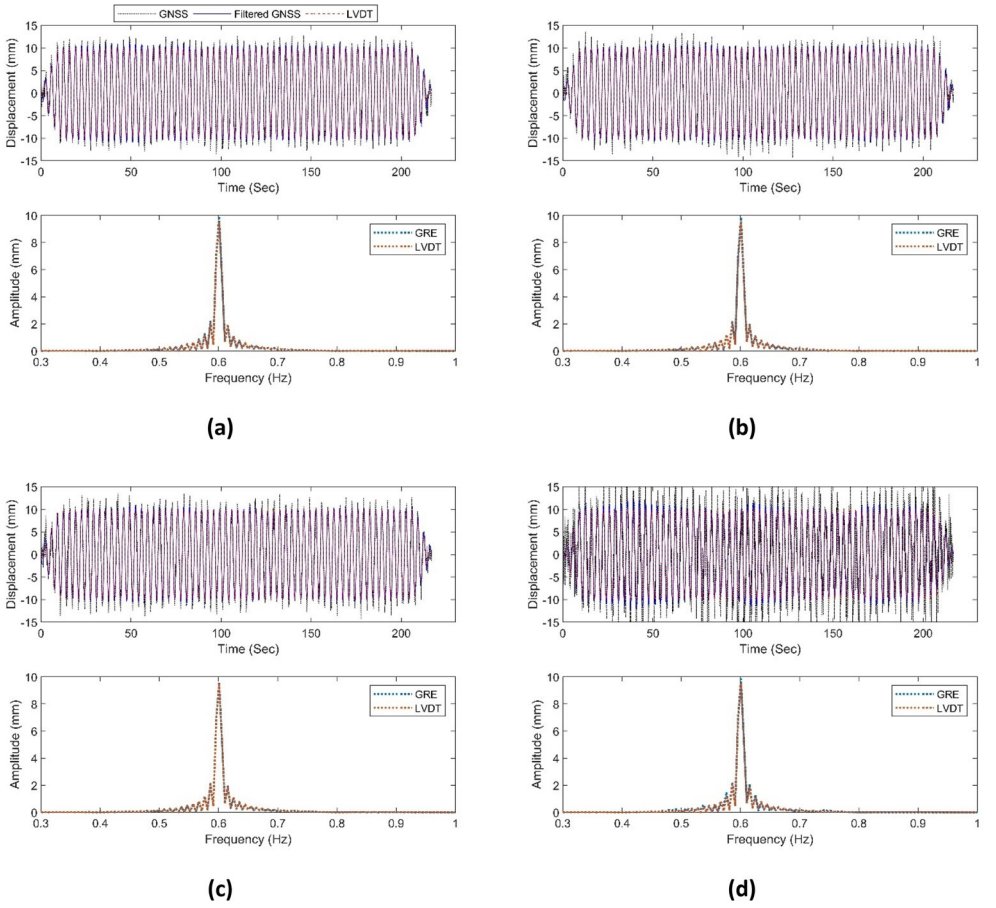

Figure 12. Performance of GPS/GLONASS/Galileo system for the event 4 dynamic case with (a) 10°, (b) 20°, (c) 30° and (d) 40° cut-off elevation angles.

off elevation angle for the four combinations provide the closest amplitude values to LVDT.

Figures 12 and 13 illustrate the performances of GPS/GLONASS and GPS/GLONASS/Galileo combinations in time and frequency domains with different cut-off elevation angles for events 4 and 3, respectively. The noise level for the 40° cut-off elevation angle results is high as shown in Figure 12. Meanwhile, the filter overcame this high noise, and the correlation between LVDT and GNSS were more than 0.99, as presented in Appendix B (see Supplementary material), Figures 10 and 12. In addition, the obtained frequencies from LVDT and GNSS were almost equal for all events when using different cut-off elevation angles, as presented in Appendix B (see Supplementary material) and Figure 12.

Finally, from the above results, it can be concluded that the accuracy of GPS/GLONASS/Galileo in the frequency domain is slightly higher than other combinations. The performance accuracy of GPS/GLONASS and GPS/GLONASS/Galileo combinations is high, and they can be used to extract the dynamic characteristics in

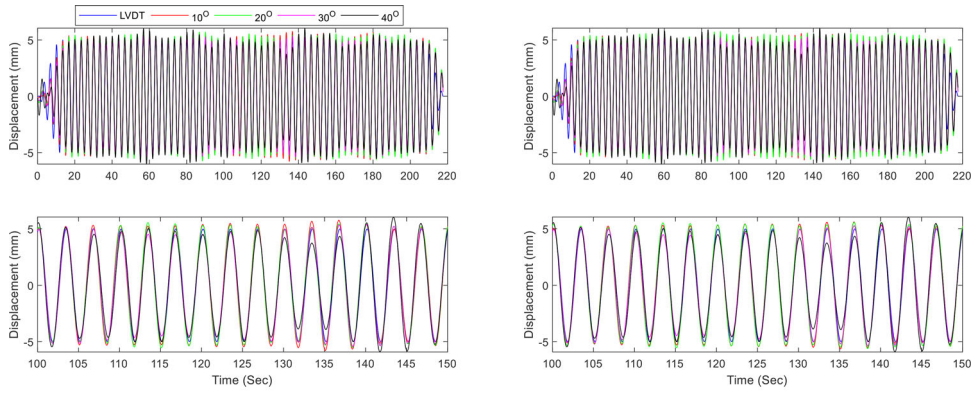

Figure 13. Correlation of (a) GPS/GLONASS and (b) GPS/GLONASS/Galileo positioning with LVDT at different cut-off elevation angles (for event 3) (top: whole data, bottom: zoom in).

the time and frequency domains. These results imply that the multi-GNSS systems with high cut-off elevation angle can make excellent benefits for monitoring structural movements in metropolitan cities.

3.4. Superimposed harmonic oscillation test

In this section, the performance of GNSS solutions was assessed for extracting three modes of structure's movements, which represent dynamic movements of three different frequencies (0.802, 3.405 and 7.613 Hz) with different amplitudes, generated by the test shake table to simulate a superimposed structural vibration. Tables 4 and 5 illustrate the performance of all GNSS combinations in time and frequency domains, respectively. Figure 14 illustrates the observed and filtered signals of GPS/GLONASS system for different cut-off elevation angles and the calculated frequencies for each event. Moreover, Figure 15 presents a comparative result of the filtered signals of the GPS/GLONASS system at the 10°, 20°, 30° and 40° cut-off elevation angles.

Table 4 shows the RMSE and SNR values of all GNSS solutions for different cut-off elevations. As can be seen from the table, like previous results, the GPS/GLONASS/Galileo combination has the smallest RMSE values and the largest SNR values for all cut-off elevation angles. These results reveal again that the triple combination system is the most accurate than GPS-only and double combinations. Moreover, GPS/GLONASS and GPS/Galileo show better performance than the GPS-only and their results are generally close to each other. Note that GPS-only did not provide a positioning solution in case of the 30° and 40° cut-off elevations. These results indicate that the double or triple satellite combinations ensure the reliable and accurate positioning even with 40° cut-off elevation. Similar to the previous harmonic events, the filter was applied to all GNSS results. The filter improved the RMSE values by 2.01%, 1.77%, 5.63% and 4.38%, on average, for all GNSS combinations, for the 10°, 20°, 30° and 40° cut-off elevation angles, respectively. Considering the SNR values, the filter decreased the noise level by 1.85%, 1.58%, 7.0%, 5.71%, on average, for all GNSS combinations, for these cut-off elevation angles, respectively. Again,

Table 4. RMSE and SNR values of all GNSS combinations ($_b$ and $_a$ denote before and after filtering).

Angle ( )	Method	$RMSE_b$ (mm)	$RMSE_a$ (mm)	SNR_b (dB)	SNR_a (dB)
10	G	2.72	2.63	8.50	8.79
	GR	2.44	2.39	9.44	9.60
	GE	2.40	2.37	9.55	9.68
	GRE	2.30	2.27	9.92	10.01
20	G	3.06	3.00	7.50	7.64
	GR	2.64	2.60	8.76	8.88
	GE	2.62	2.57	8.82	8.97
	GRE	2.45	2.40	9.40	9.53
	G	–	–	–	–
30	GR	3.32	3.10	6.80	7.40
	GE	3.07	2.91	7.48	7.93
	GRE	2.99	2.83	7.70	8.17
40	G	–	–	–	–
	GR	3.44	3.24	6.51	7.02
	GE	–	–	–	–
	GRE	2.85	2.76	8.12	8.40

Table 5. Dynamic characteristics of movements using different GNSS combinations.

		Mode 1 (Freq 0.802 Hz)		Mode 2 (Freq 3.405 Hz)		Mode 3 (Freq 7.613 Hz)	
Method	Angle (°)	Amp (mm)	Relative change (%)	Amp (mm)	Relative change (%)	Amp (mm)	Relative change (%)
LVDT	–	8.97	–	4.96	–	1.02	–
G	10	7.77	13.45	4.98	0.42	0.70	31.56
GR		7.83	12.77	5.11	2.99	0.68	32.97
GE		7.98	11.04	5.29	6.72	0.67	34.48
GRE		7.97	11.22	5.28	6.48	0.66	35.17
G	20	7.63	15.03	5.09	2.62	0.76	25.54
GR		7.87	12.26	5.25	5.91	0.71	30.28
GE		7.88	12.24	5.29	6.76	0.67	33.64
GRE		7.97	11.23	5.34	7.67	0.67	34.38
G		–	–	–	–	–	–
GR	30	8.25	8.03	5.73	15.61	0.86	15.77
GE		8.48	5.56	5.67	14.32	0.73	28.21
GRE		8.43	6.04	5.69	14.77	0.76	25.61
G		–	–	–	–	–	–
GR	40	8.59	4.30	6.17	24.55	0.88	13.50
GE		8.13	9.43	5.80	17.01	0.57	43.84
GRE		8.11	9.61	5.94	19.91	0.67	33.84

both filtered and unfiltered results reveal that the multi-GNSS systems can be accurately used to measure the movements of structures in the time domain with a 40° cut-off elevation angle.

Furthermore, the evaluation of dynamic movements shows that the frequency obtained from LVDT and multi-GNSS systems are equal at all frequency modes with different cut-off elevation angles (see Table 5). The accuracy of the integrated GNSS positioning systems for estimating the frequency models of structures movements can approach 100% for all events. For detection of the movement amplitude, from Table 5, it can be seen that the large amplitude values can be accurately detected by GNSS systems. The errors in small amplitude movements are high due to the noise level of GNSS output. Furthermore, the performance of GPS/GLONASS and GPS/

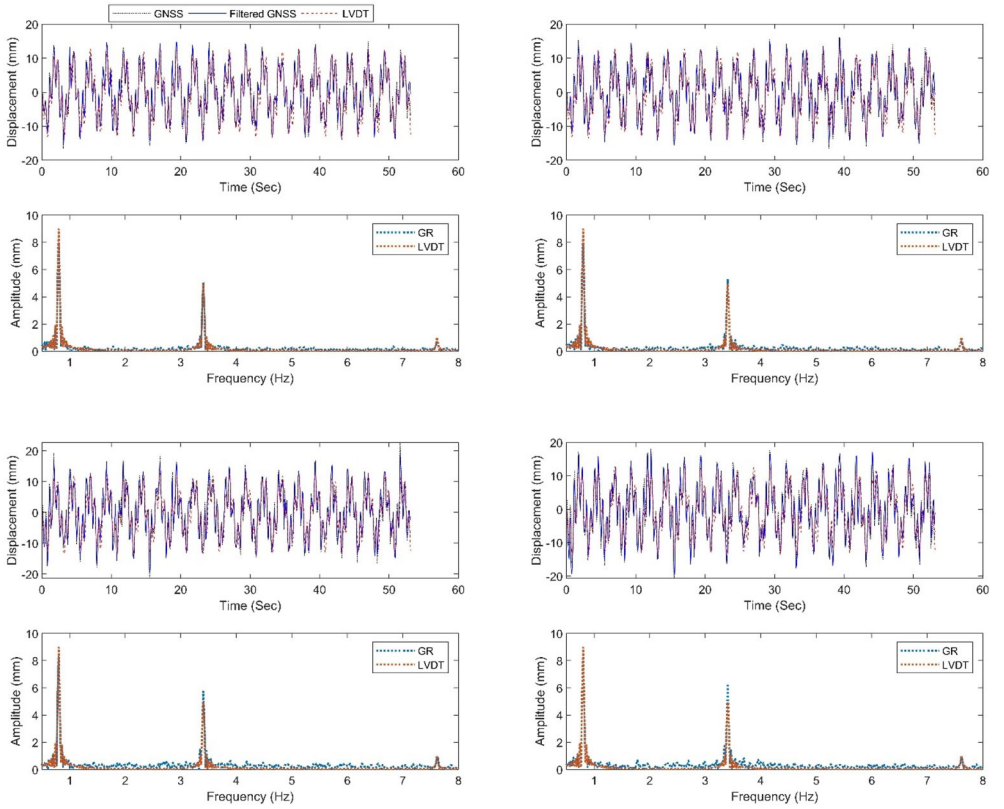

Figure 14. Performance of using GPS/GLONASS observations for extracting dynamics with (top-left) 10°, (top-right) 20°, (bottom-left) 30° and (bottom-right) 40° cut-off elevation angles.

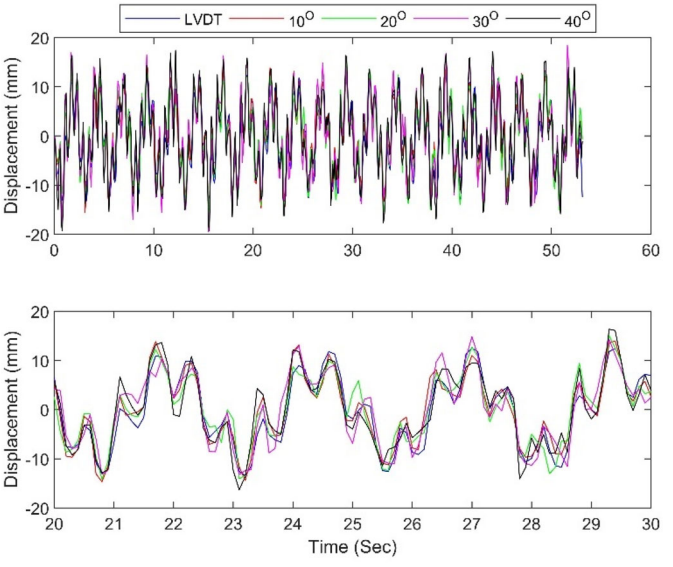

Figure 15. Comparison of the performance of different cut-off elevation angles using GPS/GLONASS (bottom: zoom in).

GLONASS/Galileo was high in extracting the dynamic amplitude of structures with average relative changes about 15% and 18%, respectively. This means that the overall accuracy of integrating GPS, Galileo and GLONASS is 82–85%. In addition, the combination of these systems always has the lowest noise level in the whole tested frequency bands. Although the best performance was observed with low-frequency modes, it is still beneficial for the high-frequency modes. In conclusion, the combination of GNSS positioning systems can improve the accuracy of monitoring structural movements up to 100% and 82% for the frequency and amplitude, respectively, comparing by LVDT measurements, at a 40° cut-off elevation angle.

4. Summary and conclusions

This study investigates, for the first time, experimentally the benefit, efficiency and usability of high-rate multi-GNSS system with high cut-off elevation angles for monitoring dynamic behaviours of engineering structures, such as high-rise or skyscrapers in urban areas, especially when surrounded by obstacles causing limited sky view and multipath errors for GNSS observations. The positioning performance of the GPS-only, GPS/Galileo, GPS/GLONASS and GPS/GLONASS/Galileo combinations were analyzed for different cut-off elevation angles, namely 10°, 20°, 30° and 40°. LVDT data was taken as the reference for time and frequency domain analyses. A processing steps for estimating accurate movements amplitudes and frequencies were proposed by using band-pass filter and FFT methods. The RMSE and the signal-to-noise ratio were computed to evaluate the accuracy of GNSS solutions in the time domain. The observed satellites during experimentation showed that the number of satellites could be decreased by 25%, 40% and 60% on average, relative to the number of satellite with cut-off angle 10°, in the cases of using 20°, 30° and 40° cut-off angles, respectively. Moreover, the PDOP evaluation showed that the best satellite position geometry under 10°, 20° and 30° elevation cut-off was obtained by using multi-GNSS observations, and the PDOP was equal on average for the GPS/GLONASS and GPS/Galileo/GLONASS under the 40° cut-off elevation angle.

According to the time-domain analysis, the results showed that the noise level and the RMSE values of all events increased with increasing the cut-off elevation angle for all unfiltered GNSS solutions. However, the noise level and RMSE of the integrated GPS/GLONASS/Galileo were smaller than GPS-only, GPS/GLONASS and GPS/Galileo for all cut-off elevation angles. In case of the 40° cut-off elevation angle, GPS/GLONASS and GPS/GLONASS/Galileo still provide positioning for all events while the GPS-only and integrated GPS/Galileo, at the time of the test with a low number of Galileo satellites, do not produce positioning solutions for some events. After filter implementation to GNSS results, the RMSE values of all satellite combinations significantly improved for all cut-off elevations. The differences between the RMSE values of the filtered GNSS results for all cut-off elevations were small when compared to that of unfiltered GNSS results. However, GPS/GLONASS/Galileo combination for all events and all cut-off elevations still provide the most accurate results after filtering (see Appendix A, see Supplementary material). The filter has improved the results of the multi-GNSS system with different cut-off elevation angles, where the accuracy of

GNSS signals for all GNSS combinations and cut-off elevation angle increased by 70%, on average, and the level of noise decreased by 110.67%, 128.47%, 238.22% and 281.29%, on average, for cut-off elevation angles 10°, 20°, 30° and 40°, respectively. As the results of both unfiltered and filtered GPS/GLONASS and GPS/GLONASS/Galileo combined systems are very promising.

A combined system would allow the use of high cut-off elevations and increases the GNSS applicability in constrained environments, where low-level multipath is present (Han et al. 2018) and can be used effectively in SHM and seismology. According to the frequency domain analysis, results demonstrated that the dominant frequencies obtained from all GNSS solutions and LVDT are very consistent with each other and were the same for all cut-off elevation angles, but there are small differences in the amplitudes ranging from 0.1 to 0.6 mm. This implies that the natural frequency of engineering structures or dynamic motion can be captured by multi-GNSS observations with high cut-off elevation angles.

Data availability

The authors confirm that the data supporting the findings of this study are available within the article and its supplementary materials.

Disclosure statement

No potential conflict of interest was reported by the authors.

Funding

This work is supported by the Basic Science Research Program through the National Research Foundation of Korea (NRF) funded by the Ministry of Science, ICT & Future Planning [2019R1I1A1A01062202]. The second author would like to thank the TUBITAK (Scientific and Technological Research Council of Turkey) Science Fellowships and Grant Programs Department for awarding him a grant to perform a research on High-rate GNSS Methods for seismology and Structural Health Monitoring Applications including this study at the School of Earth and Planetary Sciences, Curtin University, Australia.

ORCID

Mosbeh R. Kaloop http://orcid.org/0000-0002-8449-8883
Cemal O. Yigit http://orcid.org/0000-0002-1942-7667
Ahmed El-Mowafy http://orcid.org/0000-0001-7060-4123
Mert Bezcioglu http://orcid.org/0000-0001-7179-8361

References

Abedi AA, Mosavi MR, Mohammadi K. 2020. A new recursive satellite selection method for multi-constellation GNSS. Surv Rev. 52(373):330–340.
Blanco-Delgado N, Nunes FD. 2010. Satellite selection method for multi-constellation GNSS using convex geometry. IEEE Trans Veh Technol. 59(9):4289–4297.

da Silva I, Ibañez W, Poleszuk G. 2018. Experience of using total station and GNSS technologies for tall building construction monitoring. In International Congress and Exhibition "Sustainable Civil Infrastructures: Innovative Infrastructure Geotechnology". p. 471–486. https://doi.org/10.1007/978-3-319-61914-9_36.

Dabove P, Pietra V. 2019. Single-baseline RTK positioning using dual-frequency GNSS receivers inside smartphones. Sensors. 19(19):4302.

El-Mowafy A, Xu B, Hsu LT. 2020. Integrity monitoring using multi-GNSS pseudorange observations in the urban environment combining ARAIM and 3D city models. J Spat Sci. https://doi.org/10.1080/14498596.2020.1734109.

Ge Y, Zhou F, Dai P, Qin WJ, Wang S, Yang X. 2019. Precise point positioning time transfer with multi-GNSS single-frequency observations. Measurement. 146:628–642.

Gökalp E, Taşçı L. 2009. Deformation monitoring by GPS at embankment dams and deformation analysis. Surv Rev. 41(311):86–102.

Górski P. 2017. Dynamic characteristic of tall industrial chimney estimated from GPS measurement and frequency domain decomposition. Eng Struct. 148:277–292.

Guo L, Wang F, Sang J, Lin X, Gong X, Zhang W. 2020. Characteristics analysis of raw multi-GNSS measurement from Xiaomi Mi 8 and positioning performance improvement with L5/E5 frequency in an urban environment. Remote Sens. 12(4):744. https://doi.org/10.3390/rs12040744.

Han J, Huang G, Zhang Q, Tu R, Du Y, Wang X. 2018. A new azimuth-dependent elevation weight (ADEW) model for real-time deformation monitoring in complex environment by multi-GNSS. Sensors. 18(8):2473. https://doi.org/10.3390/s18082473.

Han H, Wang J, Meng X, Liu H. 2016. Analysis of the dynamic response of a long span bridge using GPS/accelerometer/anemometer under typhoon loading. Eng Struct. 122:238–250.

Kaloop MR, Elbeltagi E, Hu J, Elrefai A. 2017. Recent advances of structures monitoring and evaluation using GPS-time series monitoring systems: a review. IJGI. 6(12):382. https://doi.org/10.3390/ijgi6120382.

Kaloop MR, Kim D. 2014. GPS-structural health monitoring of a long span bridge using neural network adaptive filter. Surv Rev. 46(334):7–14.

Kaloop MR, Yigit CO, El-Mowafy A, Dindar AD, Bezcioglu M, Hu J. 2019. Hybrid wavelet and principal component analyses approach for extracting dynamic motion characteristics from displacement series derived from multipath-affected high-rate GNSS observations. Remote Sens. 12(1):79. https://doi.org/10.3390/rs12010079.

Kaloop MR, Yigit CO, Hu J. 2018. Analysis of the dynamic behavior of structures using the high-rate GNSS-PPP method combined with a wavelet-neural model: numerical simulation and experimental tests. Adv Space Res. 61(6):1512–1524.

Larocca A, Schaal R, Santos M, Langley R. 2005. Monitoring the deflection of the Pierre-Laporte suspension bridge with the phase residual method. Proceedings of the 18th International Technical Meeting of the Satellite Division of the Institute of Navigation (ION GNSS 2005), Long Beach, CA, September 2005, p. 2023–2028.

Li T, Zhang H, Gao Z, Chen Q, Niu X. 2018. High-accuracy positioning in urban environments using single-frequency multi-GNSS RTK/MEMS-IMU integration. Remote Sens. 10(2):205. https://doi.org/10.3390/rs10020205.

Liu X, Zhang S, Zhang Q, Ding N, Yang W. 2019. A fast satellite selection algorithm with floating high cut-off elevation angle based on ADOP for instantaneous multi-GNSS single-frequency relative positioning. Adv Space Res. 63(3):1234–1252.

Luo S, Wang L, Tu R, Zhang W, Wei J, Chen C. 2020. Satellite selection methods for multi-constellation advanced RAIM. Adv Space Res. 65(5):1503–1517.

Moschas F, Stiros S. 2011. Measurement of the dynamic displacements and of the modal frequencies of a short-span pedestrian bridge using GPS and an accelerometer. Eng Struct. 33(1):10–17.

Moschas F, Stiros S. 2014. Dynamic multipath in structural bridge monitoring: an experimental approach. GPS Solut. 18(2):209–218.

Olmo NQ, Martinez MJ, Abadia MF. 2016. A smart real-time monitoring GNSS system for high-rise buildings. In CTBUH 2016 Shenzhen Guangzhou. p. 1216–1226.
Ou G, Li G, Peng A. 2014. Fast satellite selection method for multi-constellation global navigation satellite system under obstacle environments. IET Radar Sonar Navig. 8(9):1051–1058.
Pan S, Meng X, Gao W, Wang S, Dodson A. 2014. A new approach for optimising GNSS positioning performance in harsh observation environments. J Navi. 67(6):1029–1048.
Paull L, Saeedi S, Seto M, Li H. 2014. AUV navigation and localization: a review. IEEE J Oceanic Eng. 39(1):131–149.
Paziewski J, Kurpinski G, Wielgosz P, Stolecki L, Sieradzki R, Seta M, Oszczak S, Castillo M, Martin-Porqueras F. 2020. Towards Galileo + GPS seismology: validation of high-rate GNSS-based system for seismic events characterisation. Measurement. 166:108236.
Paziewski J, Sieradzki R. 2017. Integrated GPS + BDS instantaneous medium baseline RTK positioning: signal analysis, methodology and performance assessment. Adv Space Res. 60(12):2561–2573.
Paziewski J, Sieradzki R, Baryla R. 2018. Multi-GNSS high-rate RTK, PPP and novel direct phase observation processing method: application to precise dynamic displacements detection. Meas Sci Technol. 29(3):035002.
Paziewski J, Sieradzki R, Baryla R. 2019. Detection of structural vibration with high-rate precise point positioning: case study results based on 100 Hz multi-GNSS observables and shake-table simulation. Sensors. 19:4832.
Ruotsalainen L, Kuusniemi H. 2013. Visual positioning in a smartphone. In: Image processing. Hershey, PA: IGI Global; p. 575–603. https://doi.org/10.4018/978-1-4666-3994-2.ch030.
Schaal R, Larocca A. 2002. Methodology for monitoring vertical dynamic sub-centimeter displacments with GPS. GPS Solut. 5(3):15–18.
Shariati M, Mafipour MS, Mehrabi P, Bahadori A, Zandi Y, Salih M, Nguyen H, Dou J, Song X, Poi-Ngian S. 2019. Application of a hybrid artificial neural network-particle swarm optimization (ANN-PSO) model in behavior prediction of channel shear connectors embedded in normal and high-strength concrete. Appl Sci. 9(24):5534. https://doi.org/10.3390/app9245534.
Shen N, Chen L, Liu J, Wang L, Tao T, Wu D, Chen R. 2019. A review of global navigation satellite system (GNSS)-based dynamic monitoring technologies for structural health monitoring. Remote Sens. 11(9):1001. https://doi.org/10.3390/rs11091001.
Shenoi BA. 2005. Introduction to digital signal processing and filter design. Hoboken, NJ: John Wiley & Sons, Inc. https://doi.org/10.1002/0471656372.
Sofi M, Lumantarna E, Zhong A, Mendis PA, Duffield C, Barnes R. 2018. Determining dynamic characteristics of high rise buildings using interferometric radar system. Eng Struct. 164:230–242.
Souza E, Negri T. 2017. First prospects in a new approach for structure monitoring from GPS multipath effect and wavelet spectrum. Adv Space Res. 59(10):2536–2547.
Takasu T, Yasuda A. 2009. Development of the low-cost RTK-GPS receiver with an open source program package RTKLIB. In International Symposium on GPS/GNSS, Jeju, Korea; p. 4–6.
Teunissen PJG, Odolinski R, Odijk D. 2014. Instantaneous BeiDou + GPS RTK positioning with high cut-off elevation angles. J Geod. 88(4):335–350.
Xi R, He Q, Xiaolin M. 2021. Bridge monitoring using multi-GNSS observations with high cutoff elevations: a case study. Measurement. 168:108303.
Xi R, Xiaolin M, Jiang W, He Q, An X. 2019. Performance analysis of bridge monitoring with the integrated GPS, BDS and GLONASS. In 4th Joint International Symposium on Deformation Monitoring (JISDM), Athens, Greece.
Yigit CO. 2016. Experimental assessment of post-processed kinematic precise point positioning method for structural health monitoring. Geomatics Nat Hazards Risk. 7(1):360–383.
Yigit CO, El-Mowafy A, Bezcioglu M, Dindar AA. 2020. Investigating the effects of ultra-rapid, rapid vs. final precise orbit and clock products on high-rate GNSS-PPP for capturing dynamic displacements. Struct Eng Mech. 73(4):427–436.

Yigit CO, Gurlek E. 2017. Experimental testing of high-rate GNSS precise point positioning (PPP) method for detecting dynamic vertical displacement response of engineering structures. Geomatics Nat Hazards Risk. 8(2):893–904.

Yu S, Guo F, Zhang X, Liu W, Li X, Wu R. 2018. A new method for GNSS multipath mitigation with an adaptive frequency domain filter. Sensors. 18(8):2514. https://doi.org/10.3390/s18082514.

Yu J, Meng X, Yan B, Xu B, Fan Q, Xie Y. 2020. Global navigation satellite system-based positioning technology for structural health monitoring: a review. Struct Control Health Monit. 27(1):e2467. https://doi.org/10.1002/stc.2467.

Zhang L, Jian L, Jin s. H, Hui Z, YouZhe X. 2013. Enhancements of the satellite selection method for multi-constellation GNSS using convex geometry. In IET International Radar Conference 2013; p. 0114–0114. https://doi.org/10.1049/cp.2013.0491.

Zhang X, Zhang Y, Li B, Qiu G. 2018. GNSS-based verticality monitoring of super-tall buildings. Appl Sci. 8(6):991. https://doi.org/10.3390/app8060991.